Fish and Shellfish Immunology 92 (2019) 54–63

Contents lists available at ScienceDirect

Fish and Shellfish Immunology

journal homepage: www.elsevier.com/locate/fsi

Full length article

The important role of phagocytosis and interleukins for nile tilapia (*Oreochromis niloticus*) to defense infection of *Aeromonas hydrophila* based on transcriptome analysis

Longgang Zhang[a,b,c], Chao Wang[a,b,c,*], Han Liu[a,b,c], Peisheng Fu[a,b,c]

[a] Shandong Freshwater Fisheries Research Institute, Jinan, 250013, China
[b] Shandong Provincial Key Laboratory of Freshwater Genetics and Breeding, Jinan, 250013, China
[c] Shandong Provincial Freshwater Aquatic Products Quality Inspection Center, Jinan, 250013, China

ARTICLE INFO

Keywords:
Tilapia
Aeromonas hydrophila
Transcriptome
Immune response
Phagocytosis

ABSTRACT

Tilapia is an important economic fish worldwide. It is vital to understand the mechanism of immune response for the prevention and treatment the infection of *Aeromonas hydrophila*. Based on high-throughput sequencing of Illumina HiSeq™, we found differentially expressed genes in the immune-related pathway were classified into phagosome, cytokine-cytokine receptor interaction and toll-like receptor signaling pathway. Gene Ontology terms were divided into three categories of transporting function, DNA replication activity and energy supply activity. The first one was related to phagocytosis and the process or transporting of antigen driven by tubulins; the second one was to differentiation and proliferation of lymphocyte activated by cytokines; and the former two both needed energy provided by the third one. According to colchicine assay, cross-immune assay, ELISA of interleukins and classical phagocytosis assay, phagocytosis and interleukins were verified to be most important to defense the infection of *A. hydrophila.*

Conflicts of interest

The authors declare no conflict of interest.

1. Introduction

Tilapia is an important economic fish all over the world, which will be one of the most providers of animal protein in the future. In China, the annual yield of tilapia is 1.7 million tons and accounts for nearly 50% of worldwide production. However, bacterial disease has strongly threatened the aquaculture of tilapia and resulted in great economic loss. *Aeromonas hydrophila* is facultative anaerobic and Gram-negative rods. It is the main pathogen of fish [1], causing hemorrhagic septicemia [2,3], and human is one of the hosts [4]. Therefore, the mechanism of immune response is important for disease prevention and public health.

Genomic sequencing, especially next-generation sequencing technologies such as the Solexa/Illumina technology [5], offers great advantages in transcriptome analysis of immune-related gene and signaling pathway [6–8]. De novo transcriptome analysis has been applied to many fish, such as *Pseudosciaena crocea*, *Epinephelus coioides*, *Lates calcarifer*, *Ctenopharyngodon idella*, *Takifugu rubripes* and so on [9–13], which was infected by bacterial, virus [14] or parasite [15]. Although there have been some transcriptome research of tilapia [16,17], the model of immune response to *A. hydrophila* of tilapia is not clear [56]. Spleen plays an important role in adaptive immune responses [18], which contains a mass of lymphocyte and macrophage. There is no report on the spleen transcriptome of tilapia in response to *A. hydrophila.* It is reasonable to choose spleen as a target tissue to reveal the mechanism of immune response to *A. hydrophila*.

In this study, we identified immune-related genes and pathways and found phagosome and interleukins was important for tilapia to defense *A. hydrophila* infection.

2. Materials and methods

2.1. Fish and bacteria

The healthy *N. tilapia* was collected from the farm of Shandong Freshwater Fisheries Research Institute in Jinan, Shandong Province, China. *A. hydrophila* was provided by Shanghai Ocean University. *Edwardsiella tarda* ATCC15947 was provided by China Center of

* Corresponding author. Shandong Freshwater Fisheries Research Institute, Jinan, 250013, China.
E-mail address: wangchao850303@163.com (C. Wang).

https://doi.org/10.1016/j.fsi.2019.05.041
Received 7 January 2019; Received in revised form 9 April 2019; Accepted 20 May 2019
Available online 29 May 2019

Industrial Culture Collection. All animals and experiments were approved by the Ethics Committee of Animal Experiments of Shandong Freshwater Fisheries Research Institute (project number is 2018082003).

The fish were acclimated for two weeks in recirculating freshwater system at 25 °C. After narcotize by MS-222, each fish (630 ± 10.2g) of infection group was challenged by intraperitoneal injection with 10^8 CFU of *A. hydrophila*, and control group was PBS. Spleen and/or plasma were collected randomly for transcriptome sequencing with six fishes of each group, or quantitative real-time PCR (qRT-PCR) validation and ELISA with three repeats.

The fish (24 ± 2.3g) were divided into three groups, twenty each. The Group 1 (G1) and Group 3 (G3) were administrated by intraperitoneal injection with 50 μg colchicine, which dissolved in 100 μL PBS, once daily for three days, and the Group 2 (G2) was injected with 100 μL PBS. On the third day, the group of G2 and G3 were challenged by intraperitoneal injection of 5×10^6 CFU/fish of *A. hydrophila*. The fish were observed twice daily for 15 days. The rest fishes were euthanized by narcotize with MS-222 and pounding head, and finally were innocuous treatment.

In the cross-immune assay, the fish (24 ± 2.3g) were divided into two groups, thirty each. The group A and B were administrated by intraperitoneal injection with 10^5 CFU/fish of *A. hydrophila* and *E. tarda*, respectively. After immune two times once a week, the two groups were challenge by *A. hydrophila* with 10^8 CFU/fish. The fish were observed twice daily for 15 days. The rest fishes were innocuous treatment as the method mentioned above.

2.2. Transcriptome sequencing

Total RNA of each group was extracted from spleen by using Trizol reagent (Invitrogen, USA), according to the manufacturer's instructions. The mRNA was purified from total RNA using poly-T oligo-attached magnetic beads. First strand cDNA was synthesized by random hexamer primer and M-MuLV Reverse Transcriptase (RNase H^-). Second strand cDNA synthesis was performed by DNA polymerase I and RNase H. After converted remaining overhangs into blunt ends and adenylation of 3′ ends of DNA fragments, NEBNext Adaptor (NEBNext Ultra™ RNA Library Prep Kit for Illumina, NEB, USA) with hairpin loop structure were ligated to prepare for hybridization. Then PCR was performed with Phusion High-Fidelity DNA polymerase, Universal PCR primers and Index (X) Primer. At last, PCR products were purified and the mixed DNA preparations were sequenced on the platform of Illumina HiSeq™.

2.3. Transcriptome data analysis

All the transcriptome analysis was based on clean data with high quality, according to the paper reported previously [19,20]. Clean data was obtained by removing adaptor sequences and low quality reads. The Q20 and GC content were calculated. Gene Ontology (GO) annotation was obtained from Blast2GO program based on NCBI non-redundant protein database. The KEGG pathways of unigenes were analyzed by blastx hits with the KEGG database [21]. BLASTX similarity searching of transcripts against NCBI database was with E-value threshold of 10^{-5}, and the annotation of GO and KEGG was refer to Danio rerio database.

2.4. Identification of differential expression analysis and enrichment analysis

Index of the reference genome was built by Bowtie (version v2.2.3) and clean reads were aligned to the reference genome by TopHat (version v2.0.12). The reads numbers mapped to each gene were counted by HTSeq (version v0.6.1). And then FPKM (expected number of Fragments Per Kilobase of transcript sequence per Millions base pairs sequenced), of each gene was calculated based on the length of the gene and reads count mapped to this gene. Differential expression analysis of the two groups was performed using the DESeq R package (version 1.18.0) [22,23]. Genes with an adjusted P-value < 0.05 and log2|(FoldChange)| > 1 were defined as difference expression.

Differentially expressed genes (DEGs) were annotated by Gene ontology (GO) functional enrichment and KEGG pathway analysis. GO enrichment analysis of differentially expressed genes was implemented by GOseq R package, and GO terms with corrected P-value < 0.05 were considered as significantly enriched. KOBAS software was used to test the statistical enrichment of differential expression genes in KEGG pathways [24].

Table 1
Statistics of transcriptomic sequences.

Sample name	Infected group	Control group
Raw reads	51932465	48281652
Clean reads	50374340	46966777
Q20(%)	96.53	95.90
GC content(%)	48.05	47.97
Total mapped	43062750(85.49%)	39810868(84.76%)
Multiple mapped	1193189(2.37%)	1001008(2.13%)
Uniquely mapped	41869565(83.12%)	38809860(82.63%)
Non-splice reads	2228041(44.23%)	20911034(44.52%)
Splice reads	19589163(38.89%)	17898826(38.11%)

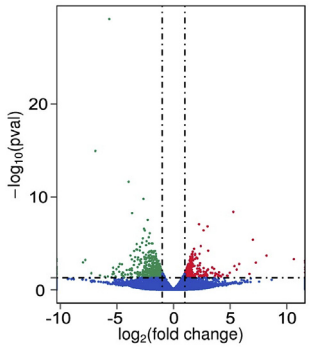

Fig. 1. Volcano plot of DEGs identified between bacteria infected group and control group. The X-axis and Y-axis represent the fold change of genetic expression in the two samples and statistics significance of differential expression, respectively. The green dots, red dots and blue dots represent genes with significantly down-regulated, up-regulated, and no significantly differential expression, respectively. (For interpretation of the references to color in this figure legend, the reader is referred to the Web version of this article.)

2.5. Quantitative real-time PCR validation

Quantitative real-time PCR (qRT-PCR) was performed to validate the DEGs of RAN-seq result. Total RNA used in qRT-PCR analysis was extracted as the method in RAN-seq. The primers were designed using Primer Premier 6.0 (Premier Biosoft, USA) and synthesized by Sangon Bothech (Shanghai) Co., Ltd (Table S1). 18S rRNA was used as the endogenous reference gene. The first-strand cDNA was synthesized from 1 μg total RNA by using PrimeScript RT Synthesis Kit (Takara Bio Inc.), according to the manufacturer's instructions. The qRT-PCR was performed with SYBR Premix Ex Taq (Takara Bio Inc.), and the cycling condition was as follows: 95 °C for 30s, 40 cycles (95 °C for 5s, 58 °C for 34s), and 72 °C for 34s. The dissolution curve temperature was 72.0–95.0 °C. All reactions were performed in triplicates. The relative expression ratio of the target genes was calculated using $2^{-\Delta\Delta CT}$ method [25], and all data were given in terms of relative mRNA expression.

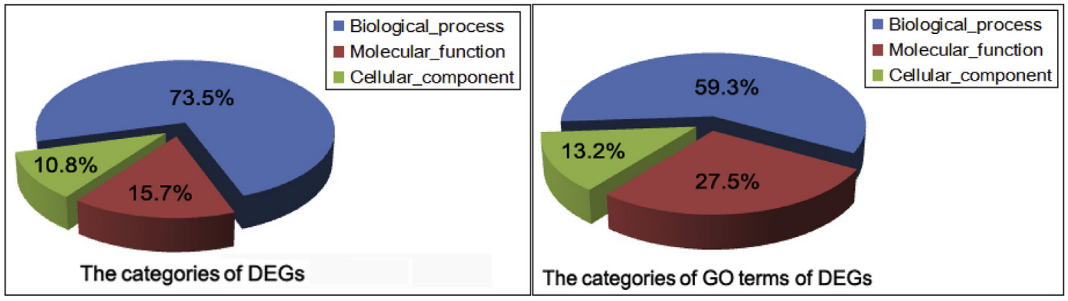

Fig. 2. The percentage of GO categories of DGEs (A) and GO terms (B). The DGEs was annotated to the three GO categories of biological process, molecular function and cellular component. Fig. 2A was the percentage of DEGs belonged to the three categories. After divided DGEs into different GO terms, percentage of these GO terms of the three categories was shown in Fig. 2B.

Table 2
Immune-related terms of GO annotation.

GO_accession	Description of GO term	Term_type	No. of DEGs
GO:0002376	immune system process	biological_process	21
GO:0006955	immune response	biological_process	17
GO:0098542	defense response to other organism	biological_process	8
GO:0009617	response to bacterium	biological_process	5
GO:0002252	immune effector process	biological_process	2
GO:0006959	humoral immune response	biological_process	2
GO:0050829	defense response to Gram-negative bacterium	biological_process	1
GO:0050776	regulation of immune response	biological_process	1
GO:0045087	innate immune response	biological_process	1
GO:0005125	cytokine activity	molecular_function	8
GO:0005126	cytokine receptor binding	molecular_function	7
GO:0042379	chemokine receptor binding	molecular_function	4
GO:0042289	MHC class II protein binding	molecular_function	2

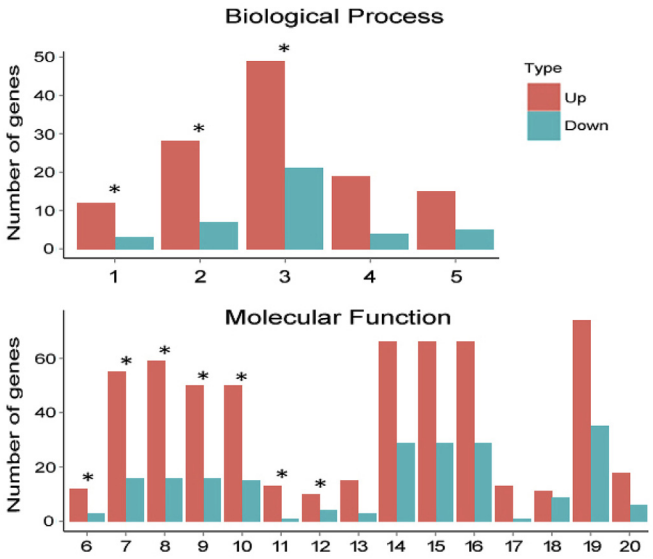

Fig. 3. The enriched GO terms of the top twenty. Y-axis represents the number of DEGs. The X-axis shows GO terms of enriched genes and the number represents: 1*, microtubule-based movement; 2*, DNA replication; 3*, DNA metabolic process; 4, movement of cell or subcellular component; 5, microtubule-based process; 6*, microtubule motor activity; 7*, hydrolase activity, acting on acid anhydrides, in phosphorus-containing anhydrides; 8*, hydrolase activity, acting on acid anhydrides; 9*, pyrophosphatase activity; 10*, nucleoside-triphosphatase activity; 11*, microtubule binding; 12*, DNA helicase activity; 13, motor activity; 14, ATP binding; 15, adenyl ribonucleotide binding; 16, adenyl nucleotide binding; 17, tubulin binding; 18, helicase activity; 19, carbohydrate derivative binding; 20, macromolecular complex binding. * The significantly enriched GO terms (p-value < 0.05).

2.6. The ELISA assay of IL-1β, IL6 and IL7

The fish was prepared as the method mentioned above. Plasma and spleen were collected at 24 h post infection with three biological repeats. Plasma was collected with heparin as an anticoagulant. After centrifuged for 20 min at the speed of 3000 rpm, the supernatant was collected. Spleen was cutted into pieces and frozen with liquid nitrogen. After homogenized, tissue samples were centrifuged for 20 min at the speed of 3000 rpm, and the supernatant was collected. Interleukins were measured using Fish IL1β, IL6 or IL7 ELISA Kit (Enzyme-linked Biotechnology Co., China) as procedure of the Kits, respectively.

2.7. Phagocytosis assay

The feeding conditions and immune dosage of bacteria of the fish was the same as cross-immune assay. The macrophage of spleen was isolated as previously described [26]. Briefly, spleens were aseptically extracted, pushed through a metal mesh and suspended in RPMI 1640 with 2% fetal bovine serum, heparin (20U/mL), penicillin (100U/mL) and streptomycin (100 μg/mL) from the control group, *A. hydrophila* infected group (Group I) and *E. tarda* infected group (Group II). The suspensions were then loaded onto a 34/51% discontinuous Percoll density gradient and centrifuged at 400 × *g* for 30 min. Cells were collected from the interphase, washed twice and adjusted to 10^7 cells/mL in RPMI 1640 with 0.1% FBS and antibiotics. After 2 h at 28 °C, non-adherent cells were washed off and the medium was changed to complete medium with 5% FBS for overnight incubation. The monolayer was washed once and covered with 200 μL RPMI 1640 with 5% FBS and 20 μL bacterial suspensions (10^8 cells, MOI = 10). After 1 h incubation, the extracellular bacteria were washed off by RPMI 1640 and the cells were transferred to sterile glass slide by 100 μL RPMI 1640. After macrophages were fixed by 100 μL methanol, the cells and bacteria were dyed by 100 μL Wright's stain, and counted under the microscope. All groups were performed in triplicates. Phagocytic ratio (PR) and phagocytic index (PI) was calculated according to the following formula:

PR = No. of macrophage with engulfed bacteria/No. of macrophage × 100%
PI = No. of engulfed bacteria/No. of phagocytic macrophage

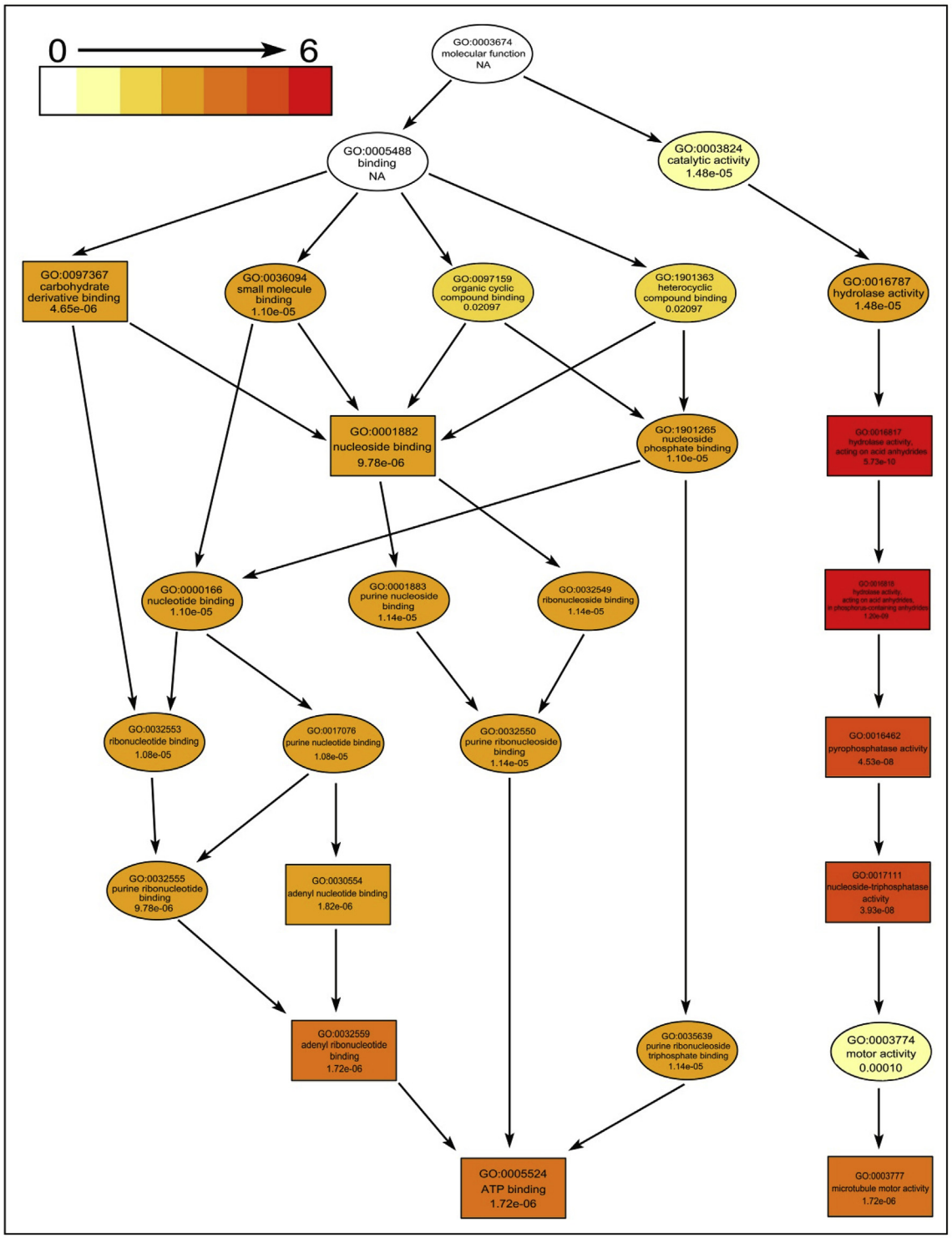

A

Fig. 4. The DAG of GO enrichment analysis of DEGs for (A) molecular function, and (B) biological process. Each node represented a GO term. The branch represented inclusion relation, and the functional range of branch was decreased gradually from top to bottom. The gradation of color represented the degree of enrichment, and the deeper color was the higher enrichment degree. Each node contained the name of GO term and p-value of enrichment analysis. (For interpretation of the references to color in this figure legend, the reader is referred to the Web version of this article.)

3. Results

3.1. RNA-seq and transcriptome sequence assembly

According to the high-throughput sequencing of Illumina HiSeq™, there were 51932465 and 48281652 raw reads of infected group and control group, respectively (Table 1). After filtering dirty reads, 50374340 and 46966777 clean reads were obtained respectively. Q20% (the value of Phred was more than 20) was over 95%, and GC percentage was nearly 48% (Table 1). The total mapped sequence

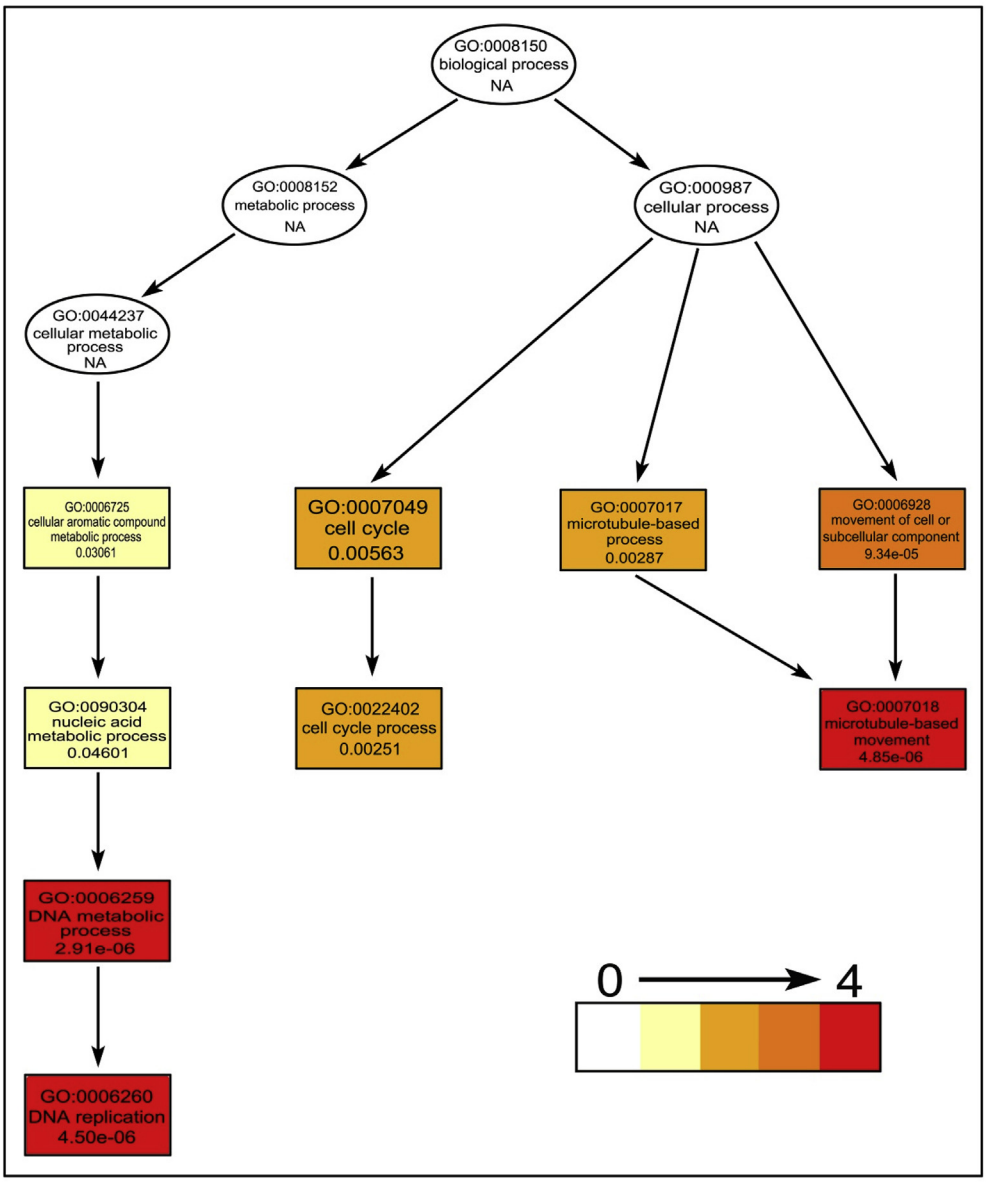

B

Fig. 4. (*continued*)

located in genome was nearly 85%. The uniquely mapped sequence, which was sole in reference sequence, was more than 82%, and multiple mapped sequence was nearly 2%. The sequence located in one exon was nearly 44% and that in two exons was nearly 39% (Table 1). There were a total of 30341 unigenes from the above two groups.

3.2. GO analysis of differentially expressed gene

There were 905 differentially expressed genes (DEGs), including 396 up-regulated genes and 509 down-regulated genes (Fig. 1). But in this report, the research was focus on the DEGs of immune related.

Gene Ontology is generally used to categorize genes and their products across species [27]. The 905 DGEs belonged to different GO categories of biological process, molecular function or cellular component. The most one was biological process (73.5%); the second one was molecular function (15.7%); and the third one was cellular component (10.8%). The GO terms could contain one or more DEGs, and the result of percentage of GO terms was similar that the former one. There were 59.3%, 27.5 and 13.2% in the biological process, molecular function and cellular component, respectively.

According to GO enrichment analysis, the DEGs of immune-related were divided into two categories of biological process and molecular function (Table 2.). The GO terms of DEGs were mainly included in immune process or immune response (GO:0002376, GO:0006955, GO:0002252 and GO:0050776), cytokine related terms (GO:0005125, GO:0005126 and GO:0042379) and defense response to bacterium (GO:0098542, GO:0009617 and GO:0050829). Immune system process (21 DEGs) and immune response (17 DEGs) were the most two terms of them (Table 2.).

The enriched GO terms of the top twenty were also in the two categories of biological process and molecular function (Fig. 3). The enriched GO terms could be divided into three categories of microtubule-related transporting (No. 1, 4, 5, 6, 11, 13 and 17), DNA replication activity (No. 2, 3, 12, 15, 16 and 18) and energy supply activity (No. 7, 8, 9, 10 and 14).

The directed acyclic graph (DAG) was graphical presentation of GO enrichment analysis of DEGs (Fig. 4), and it showed branch network of molecular function (Fig. 4A) or biological process (Fig. 4B). The former

Table 3
List of DEGs related to immune response in significant difference pathway.

Category and gene name	Gene symbol	log2FoldChange	p-value
Phagosome			
Cytoplasmic dynein	Dynein	1.13	2.88E-02
Tubulin alpha-1A	TUBA	1.34	1.59E-03
Calreticulin	CALR	1.25	1.45E-02
Tubulin beta chain	TUBB	1.38	2.35E-02
Cathepsin L1	Cathepsin	1.62	4.75E-02
Macrophage mannose receptor 1	MR	2.39	1.14E-02
Major histocompatibility complex class II	MHCII	1.71	7.88E-03
Major histocompatibility complex class I	MHCI	−1.97	3.33E-03
Toll-like receptor 2 type-1	TLR2	1.48	5.71E-04
Cytokine-cytokine receptor interaction			
Receptor-type tyrosine-protein kinase FLT3-like isoform X4	FLT3	−4.28	2.34E-02
Chemokine XC receptor 1	XCR1	1.18	2.54E-02
C–C motif chemokine 3	CCL3	−1.39	1.71E-02
C–C motif chemokine 20-like	CCL20	−2.75	4.79E-02
Mast/stem cell growth factor receptor Kit	KIT	−2.56	4.93E-04
Platelet-derived growth factor receptor alpha	FDGFRA	−2.18	1.09E-02
Tumor necrosis factor ligand superfamily member 10	TNFSF10	−1.64	1.01E-02
Tumor necrosis factor ligand superfamily member 14	TNFSF14	1.61	1.96E-02
Tumor necrosis factor receptor superfamily member 11B-like isoform X3	SF11B	−1.61	2.31E-02
Interleukin-7 receptor subunit alpha	IL7R	1.07	3.96E-02
Interleukin-1 beta-like isoform X1	IL1β	1.40	4.41E-02
Interleukin-6	IL6	1.46	4.93E-02
Toll-like receptor signaling pathway			
Toll-like receptor 2 type-1	TLR2	1.48	5.71E-04
Interleukin-1 beta-like isoform X1	IL-1β	1.40	4.41E-02
Interleukin-1 receptor type 1	IL1R1	2.06	5.97E-03
Interleukin-1 receptor type 2	IL1R2	2.42	1.57E-05
Dual specificity mitogen-activated protein kinase kinase 7	MKK4/7	−1.88	7.12E-03
Toll-like receptor 5	TLR5	1.27	7.35E-03
Transcription factor AP-1	AP-1	1.66	4.80E-02
Others			
Immunoglobulin mu heavy chain	IgM	3.06	6.05E-05
Fos-related antigen 2	Fosl2	1.91	1.39E-04
Membrane-associated form by triggering lysosome-dependent degradation	TMEM131L	−1.33	4.15E-03
phospholipid-transporting ATPase IM	ATP8B4	1.17	8.24E-03
Serine/threonine-protein kinase Chk1	CHEK1	1.70	1.71E-03

one pointed to ATP binding and microtubule motor activity. The latter one was to DNA replication and microtubule-based movement. It is similar to enriched GO terms and it also could be divided into three categories of microtubule-related transporting, DNA replication activity and energy supply activity.

3.3. KEGG analysis of differentially expressed genes

In KEGG analyses, 905 DEGs were annotated within 108 pathways and the most significantly enriched pathway were DNA replication, cell cycle and phagosome. But the pathways, related to immune response directly, were classified into three categories of phagosome, cytokine-cytokine receptor interaction and Toll-like receptor signaling pathway (Table 3).

3.4. Pathway analysis

Phagosome pathway was the most significantly enriched pathway related to immune response, which contains 9 DEGs (Table 3) and all of them were up-regulated except for MHCI. The phagosome pathway (Fig. 5) was drawn based on the database of KEGG (http://www.kegg.jp/). The six proteins, Dynein, TUBA, TUBB, CALR, cathepsin and MR, participated directly in process of antigen endocytosis, and the other two proteins, MHCI and MHCII, were molecular of antigen presentation.

3.5. Quantitative real-time PCR analysis

Six DEGs related to immune response were selected for qRT-PCR validation. The six genes belong to three categories of phagosome (Dynein, TUBA, TUBB and TLR2), cytokine-cytokine receptor interaction (XCR1) and Toll-like receptor signaling pathway (TLR2 and AP-1). qRT-PCR results showed that the six genes were all up-regulated, and they were correlated with the RNA-Seq. The fold changes of these genes were compared with the RNA-Seq expression profiles shown in Fig. 6.

3.6. Infection of *A. hydrophila* increase the content of IL-1β, IL6 and IL7 in plasma and spleen

To validate the important role of interleukins in the infection of *A. hydrophila*, the content of interleukins was measured using ELISA. In plasma and spleen, IL-1β, IL6 and IL7 were all significantly increased, except for IL7 in plasma (Fig. 7). The result was consistent with transcriptome sequencing.

3.7. The validation assay of colchicine and cross-immune

Tubulin was important in phagocytosis, which was up-regulated in the infection of *A. hydrophila* (Table 3). To certify the role of tubulin in process of bacterial infection, tilapia were injected with colchicine and challenged with *A. hydrophila*. Under the influence of colchicine, the survival rate was decreased from 75% to 35% ($P < 0.05$) (Fig. 8A). The inhibition of microtubule polymerization by colchicine could impair the defense capability of tilapia against *A. hydrophila*.

The cross-immune assay was aimed to validate the important role of phagocytosis, considering *E. tarda* could activate phagocytosis pathway [28]. After the two times immune of *A. hydrophila* or *E. tarda*, the survival rate of the two groups was similar, which was 63.3% and 53.3%, respectively (Fig. 8B), and there was no significant difference.

3.8. Phagocytosis was activated by A. hydrophila

After immune with *A. hydrophila* or *E. tarda*, the PR and PI were both increased significantly in the phagocytosis of *A. hydrophila* (Fig. 9). The PR of Control group, Group I and Group II was 14.3%, 23.5% and 27.2%, respectively. The PI in the three groups above was 1.87, 2.76 and 2.98, respectively. The phagocytic efficiency after immune with *E. tarda* (Group II) was even higher than Group I (*A. hydrophila* infected group), but there was no significance between each other.

4. Discussion

High-throughput sequencing makes it convenience for genome and transcriptome research [29]. In this study, we got a total of 30341 unigenes from control group and bacteria infected group challenged by *A. hydrophila*. There were 905 DEGs, including 396 up-regulated genes and 509 down-regulated genes. GO enrichment analysis showed that the DGEs could be divided into three categories of microtubule-related transporting, DNA replication activity and energy supply activity. The significant pathways of KEGG analysis related to immune response were mainly divided into three categories of phagosome pathway, cytokine-cytokine receptor interaction and toll-like receptor signaling pathway. In this paper, we focused on these GO terms and pathways, which had closely associated with infection of *A. hydrophila*.

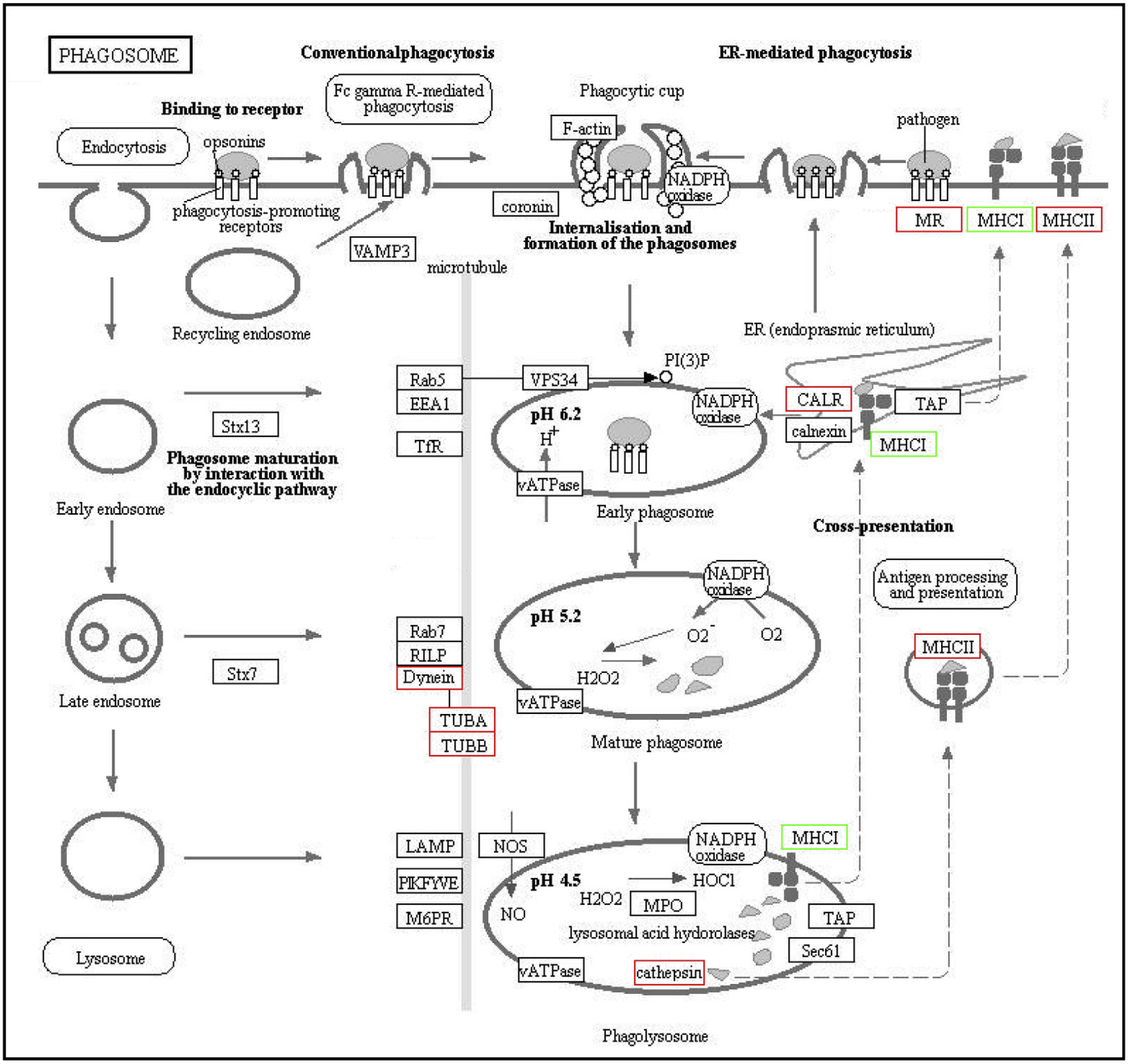

Fig. 5. The signaling pathway of phagosome mapped by KEGG. The up-regulated and down-regulated genes were marked by red and green box, respectively. (For interpretation of the references to color in this figure legend, the reader is referred to the Web version of this article.)

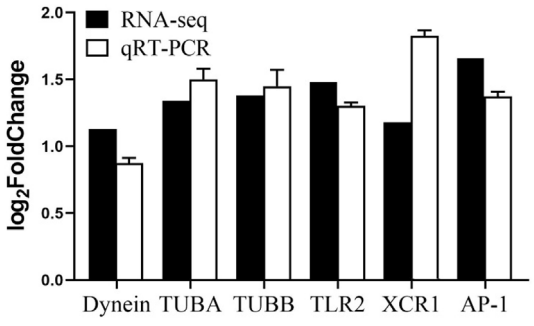

Fig. 6. Comparison of relative fold change of RNA-Seq and qRT-PCR. The expression levels of these genes were normalized by 18s RNA.

Cytokines include interleukins, chemokines, interferons, and tumour necrosis factors. The IL-1β is an important mediator of the inflammatory response, and it is participant in cell proliferation and differentiation [30]. IL6 could be secreted by macrophages in response to bacterial infection as pathogen-associated molecular patterns, which could bind to toll-like receptors, and start the production of inflammatory cytokine [31]. IL7 stimulates the differentiation and proliferation of lymphocyte [32]. During the infection of *A. hydrophila*, the IL-1β, IL6 and IL7 were all significantly increased in plasma and spleen, except for IL7 in plasma, in ELISA assay. IL-1β and IL6 was shown to be up-regulated in the infection of *A. hydrophila* [33], but IL7 was not mentioned. The number of down-regulated DEGs of chemokine and TNF was more than up-regulated ones. The XCR1 [34] and CCL3 [35] has been reported to be up-regulated and down-regulated, respectively, after the infection of *A. hydrophila*, which is accordance with this report. It was suggested that interleukins were much more important than

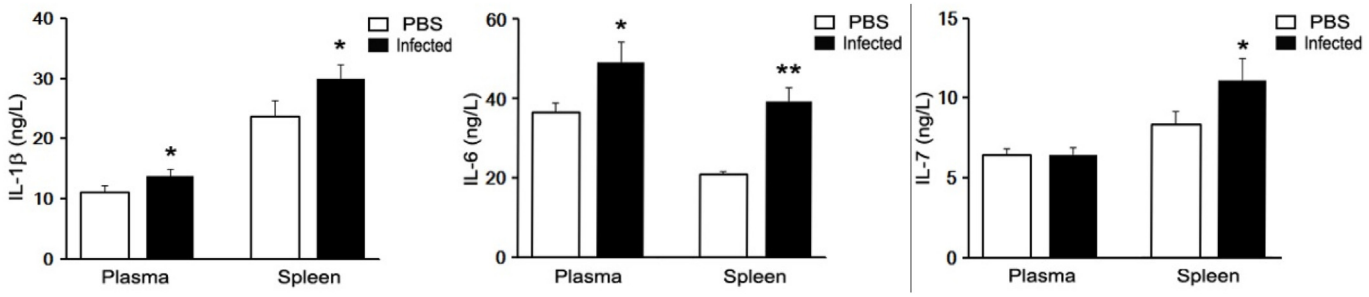

Fig. 7. The effect of *A. hydrophila* to IL-1β, IL6 and IL7 in plasma and spleen.

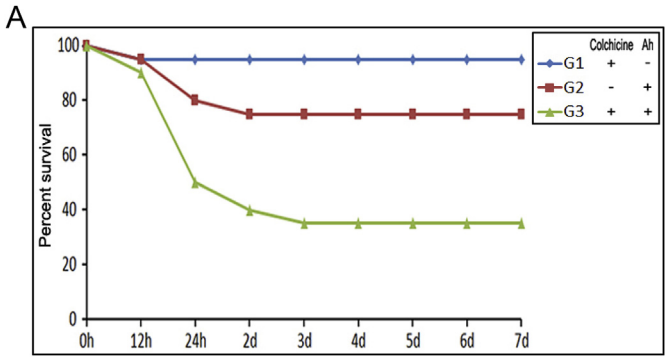

Fig. 8. A Percent survival of tilapia challenged by *A. hydrophila* with Colchicine. B Cross-immune of tilapia challenged by *A. hydrophila* or *E. tarda.*

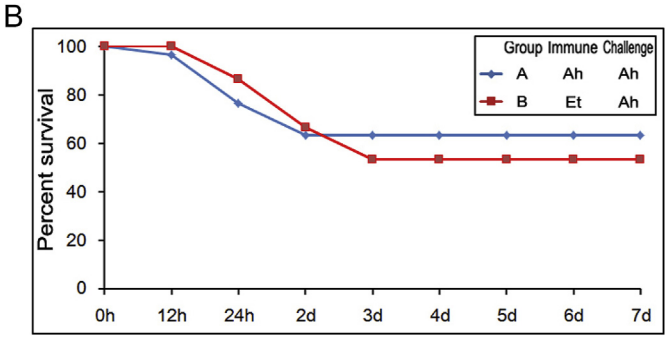

Fig. 8. (*continued*)

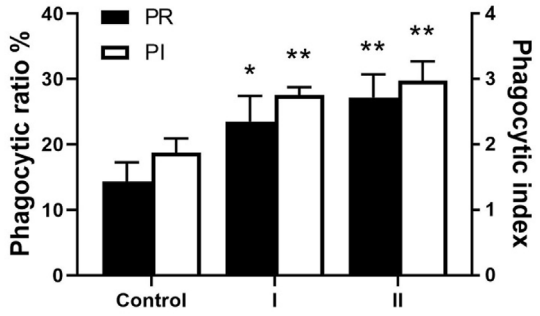

Fig. 9. The histogram of phagocytic ratio and phagocytic index. */**, P-value < 0.05/0.01 compared with control group.

chemokines and TNFs for tilapia to defense the infection of *A. hydrophila.*

Toll-like receptors (TLRs), which are expressed on macrophages and dendritic cells (DCs), are important membrane-spanning proteins. They recognize conserved molecules of microbes and activate immune cell response [36]. TLRs play a crucial role in fish immunity [37,38]. After activated, they promote the production of IL and TNF, which could regulate the Th1 and Th2 cell [39]. TLR2 recognizes bacterial and viral, which take part in the phagocytosis, and it has been found expression increased after infected by *Edwardsiella ictulari* [40], *Vibrio alginolyticus* [41] or *S. dysgalactiae* [42]. TLR5 recognizes conserved regions of flagellin, and the up-regulated expression has been observed in the infection of *Yersinia ruckeri* O1 or *A. hydrophila* [18,35]. AP-1, as a transcription factor, activates gene expression responding to cytokines, growth factors, stress, and bacterial infections [43] and it also regulates the cellular process of differentiation and proliferation [44]. IL-1β and IL-6 is activated by AP-1 in Toll-like receptor signaling pathway of KEGG, so cell proliferation and differentiation is promoted and then production of inflammatory cytokine is started.

Phagocytes are including macrophages, neutrophils, and DCs. In this study, the phagosome pathway was the most significant one related to immune response directly, including dynein, TUBA, TUBB, CALR, Cathepsin, MR, TLR2, MHCI and MHCII (Table 3), which of them was important for phagocytosis. After the receptors activated by pathogens (MR or TLR2), the compound of receptor-pathogen is swallowed by phagocytes and phagosome formed, which moves along microtubules [45,46]. Microtubules polymerized by α- and β-tubulins (TUBA and TUBB), which is a major component of the cytoskeleton [47]. Dynein is a cytoskeletal motor protein which moves along microtubules. It provides energy to transports various cellular cargos, such as endoplasmic reticulum (ER) and lysosomes [48], and it also force the displacement of chromosomes in mitosis [49,50]. Phagosome is fused with lysosome into mature phagolysosome, in which pathogens are digesting into antigen peptides with the help of cathepsins [51]. Antigen peptides are assembled into MHC compound in ER, and CALR take part in this process as a molecular chaperone. MHC compound is transported by ER and Golgi body and presented on the surface of cell [52]. MHCI activates cytotoxic T lymphocytes, which mediate cellular immunity and mean to kill viruses or some intracellular bacteria. MHCII induces Th cell to differentiate into memory Th cell or effector Th cell, and mediate the secretion of antibody and cytokines related to humoral immune [55]. MHCII is more important than MHCI for tilapia to defense the infection of *A. hydrophila*. Phagosome pathway is a hub in immune response and bridging the gap between innate and adaptive immunity [53].

In the colchicine, cross-immunoprotection and classical phagocytosis assay, the important role of phagocytosis was verified. Colchicine could disturbed phagocytosis by inhibiting microtubule polymerization, and the survival rate was decreased significantly from 75% to 35% (Fig. 8A). Phagocytosis is crucial for the host to defense the invasion of bacteria, especially for the intracellular bacterium [7]. The increased PR and PI proved that phagocytosis was activated in the similar extent after reinfection by *A. hydrophila* or *E. tarda* (Fig. 9), which maybe result in the similar protective effect between each other (Fig. 8B). *E. tarda* could activate phagocytosis pathway and MHCI antigen processing pathway, but not MHCII [28]. When the phagocytosis was activated by *A. hydrophila* even by intracellular bacterium, such as *E. tarda*, the effect of immunoprotection was similar, whether the cellular

immunity was activated by MHCI or MHCII.

The up-regulated genes of immune-related were more than down-regulated ones in enriched GO terms. The immune response was not an independent metabolic activity in host, so the focus should not be limited in immune reaction itself. From GO enrichment analysis, the top twenty terms were mainly divided into three categories, transporting function, DNA replication activity and energy supply activity. The first category was involved in the process of phagocytosis (TUBA, TUBB and Dynein). The second one was participated in DNA replication and transcription. Antigens could activate proliferation of lymphocyte, and it meant the DNA replication was more active [54]. The third one was related in hydrolyzing ATP and providing energy for microtubule-based movement involved in the process of immune response and DNA replication. So, in the DAG of GO enrichment analysis of DEGs, the molecular function was pointed to ATP binding and microtubule motor activity, and biological process was to DNA replication and microtubule-based movement, which of them were important for host to defense the challenge of *A. hydrophila*.

5. Conclusions

In this study, we performed the transcriptomic profile of tilapia in response to *A. hydrophila* infection by using high-throughput sequencing of Illumina HiSeq™. The DEGs in the immune-related pathway were classified into three of phagosome, cytokine-cytokine receptor interaction and toll-like receptor signaling pathway. According to analysis of enriched GO terms, the three categories related to infection of *A. hydrophila* were of transporting function, DNA replication activity and energy supply activity. The most important found was that phagocytosis and interleukins were important for tilapia to defense *A. hydrophila*.

Acknowledgments

This work was financially supported by Shandong Provincial Natural Science Foundation of China (ZR2018PC028); The Fish Innovation Team of Shandong Agriculture Research System (SDAIT-12-01); Agricultural Seed Project of Shandong Province (2014lz042); Shandong Provincial Key R&D Program of China (2016GNC110026); Key Research Project of Shandong Province (2018GNC110034).

Appendix A. Supplementary data

Supplementary data related to this article can be found at https://doi.org/10.1016/j.fsi.2019.05.041.

References

[1] R. Seshadri, S.W. Joseph, A.K. Chopra, et al., Genome sequence of Aeromonas hydrophila ATCC 7966T: jack of all trades, J. Bacteriol. 188 (23) (2006) 8272–8282.
[2] L.J. He, L.K. Liao, J.F. Yuan, H.Y. Tang, Q. Wu, G.W. Zhang, Pathological observation of bacterial septicemia in Megalobrana amblycephala, J Southwest Agric Univ Nat Sci 28 (3) (2006) 483–490.
[3] L. Liu, Y.X. Gong, B. Zhu, G.L. Liu, G.X. Wang, F. Ling, Effect of a new recombinant Aeromonas hydrophila vaccine on the grass carp intestinal microbiota and correlations with immunological responses, Fish Shellfish Immunol. 45 (1) (2015) 175–183.
[4] W.A. Agger, J. McCormick, M.J. Gurwith, Clinical and microbiological features of Aeromonas hydrophila-associated diarrhea, J. Clin. Microbiol. 21 (6) (1985) 909–913.
[5] Z. Wang, M. Gerstein, M. Snyder, RNA-Seq: a revolutionary tool for transcriptomics, Nat Rev Gent 10 (1) (2009) 57–63.
[6] G. Li, Y. Zhao, Z. Liu, et al., De novo assembly and characterization of the spleen transcriptome of common carp (Cyprinus carpio) using Illumina paired-end sequencing, Fish Shellfish Immunol. 44 (2) (2015) 420–429.
[7] L.J. Zhao, J.G. Tu, Y.L. Zhang, et al., Transcriptomic analysis of the head kidney of Topmouth culter (Culter alburnus) infected with Flavobacterium columnare with an emphasis on phagosome pathway, Fish Shellfish Immunol. 57 (2016) 413–418.
[8] P.P. Wang, J. Wang, Y.Q. Su, et al., Transcriptome analysis of the Larimichthys crocea liver in response to Cryptocaryon irritans, Fish Shellfish Immunol. 48 (2016) 1–11.
[9] J.H. Xia, G.H. Yue, Identification and analysis of immune-related transcriptome in Asian seabass Lates calcarifer, BMC Genomics 11 (2010) 356.
[10] Y. Mu, F. Ding, P. Cui, et al., Transcriptome and expression profiling analysis revealed changes of multiple signaling pathways involved in immunity in the large yellow croaker during Aeromonas hydrophila infection, BMC Genomics 11 (1) (2010) 506.
[11] Y. Huang, X. Huang, Y. Yan, J. Cai, Z. Ouyang, H. Cui, et al., Transcriptome analysis of orange-spotted grouper (Epinephelus coioides) spleen in response to Singapore grouper iridovirus, BMC Genomics 12 (2011) 556.
[12] J. Chen, C. Li, R. Huang, F.K. Du, L.J. Liao, Z.Y. Zhu, et al., Transcriptome analysis of head kidney in grass carp and discovery of immune-related genes, BMC Vet. Res. 8 (2012) 108.
[13] J. Cui, H. Wang, S. Liu, et al., Transcriptome analysis of the gill of Takifugu rubripes using Illumina sequencing for discovery of SNPs, Comp Biochem Physiol D Genomics Proteomics 10 (2014) 44–51.
[14] M.K. Purcell, I.S. Marjara, W. Batts, et al., Transcriptome analysis of rainbow trout infected with high and low virulence strains of Infectious hematopoietic necrosis virus, Fish Shellfish Immunol. 30 (2010) 84–93.
[15] S. Castellanos-Martinez, D. Arteta, S. Catarino, et al., De Novo transcriptome sequencing of the Octopus vulgaris hemocytes using Illumina RNA-Seq Technology: response to the infection by the gastrointestinal parasite Aggregata octopiana, PLoS One (2014) e107873.
[16] W.J. Tao, J. Yuan, L.Y. Zhou, L.N. Sun, Y.L. Sun, S.J. Yang, et al., Characterization of gonadal transcriptomes from Nile tilapia (Oreochromis niloticus) reveals differentially expressed genes, PLoS One 8 (5) (2013) e63604.
[17] R. Zhang, L.L. Zhang, X. Ye, Y.Y. Tian, C.F. Sun, M.X. Lu, et al., Transcriptome profiling and digital gene expression analysis of Nile tilapia (Oreochromis niloticus) infected by Streptococcus agalactiae, Mol. Biol. Rep. 40 (2013) 5657–5668.
[18] M.K. Raida, K. Buchmann, Development of adaptive immunity in rainbow trout, Oncorhynchus mykiss (Walbaum) surviving an infection with Yersinia ruckeri, Fish Shellfish Immunol. 25 (2008) 533–541.
[19] A. Conesa, S. Gotz, J.M. García-Gomez, et al., Blast2GO: a universal tool for annotation, visualization and analysis in functional genomics research, Bioinformatics 21 (18) (2005) 3674–3676.
[20] M.G. Grabherr, B.J. Haas, M. Yassour, et al., Full-length transcriptome assembly from RNA-Seq data without a reference genome, Nat. Biotechnol. 29 (7) (2011) 644–652.
[21] M. Kanehisa, S. Goto, KEGG: kyoto encyclopedia of genes and genomes, Nucleic Acids Res. 28 (1) (2000) 27–30.
[22] L. Wang, Z. Feng, X. Wang, X. Wang, X. Zhang, DEGseq: an R package for identifying differentially expressed genes from RNA-seq data, Bioinformatics 26 (1) (2010) 136–138.
[23] Y. Yang, M. Xu, Q. Luo, J. Wang, H. Li, De novo transcriptome analysis of Liriodendron chinense petals and leaves by Illumina sequencing, Gene 535 (2) (2014) 155–162.
[24] X. Mao, T. Cai, J.G. Olyarchuk, L. Wei, Automated genome annotation and pathway identification using the KEGG orthology (KO) as a controlled vocabulary, Bioinformatics 21 (19) (2005) 3787–3793.
[25] K.J. Livak, T.D. Schmittgen, Analysis of relative gene expression data using real-time quantitative PCR and the $2^{-\Delta\Delta CT}$ method, Methods 25 (2001) 402–408.
[26] Y.Q. He, J. Chen, X.J. Lu, et al., Characterization of P2X7R and its function in the macrophages of ayu, Plecoglossus altivelis. PLoS One 8 (2) (2013) e57505.
[27] M. Ashburner, C.A. Ball, J.A. Blake, et al., Gene ontology: tool for the unification of biology. The Gene Ontology Consortium, Nat. Genet. 25 (2000) 25e29.
[28] D. Yang, Q. Liu, C. Ni, et al., Gene expression profiling in live attenuated Edwardsiella tarda vaccine immunized and challenged zebrafish: insights into the basic mechanisms of protection seen in immunized fish, Dev. Comp. Immunol. 40 (2) (2013) 132–141.
[29] M.L. Metzker, Sequencing technologies – the next generation, Nat. Rev. Genet. 11 (2010) 31–46.
[30] M. Sahoo, I. Ceballos-Olvera, L. del Barrio, F. Re, Role of the inflammasome, IL-1β, and IL-18 in bacterial infections, Sci. World J. 11 (2011) 2037–2050.
[31] P.C. Heinrich, I. Behrmann, S. Haan, H.M. Hermanns, et al., Principles of interleukin (IL)-6-type cytokine signalling and its regulation, Biochem. J. 374 (2003) 1–20.
[32] S.A. Corfe, C.J. Paige, The many roles of IL-7 in B cell development; mediator of survival, proliferation and differentiation, Semin. Immunol. 24 (3) (2012) 198–208.
[33] Y. Jiang, S. Feng, S. Zhang, et al., Transcriptome signatures in common carp spleen in response to Aeromonas hydrophila infection, Fish Shellfish Immunol. 57 (2016) 41–48.
[34] Y. Yang, H. Yu, H. Li, A.L. Wang, Transcriptome profiling of grass carp (Ctenopharyngodon idellus) infected with Aeromonas hydrophila, Fish Shellfish Immunol. 51 (2016) 329–336.
[35] N.T. Tran, Z.X. Gao, H.H. Zhao, et al., Transcriptome analysis and microsatellite discovery in the blunt snout bream (Megalobrama amblycephala) after challenge with Aeromonas hydrophila, Fish Shellfish Immunol. 45 (2015) 72–82.
[36] Y. Palti, Toll-like receptors in bony fish: from genomics to function, Dev. Comp. Immunol. 35 (12) (2011) 1263–1272.
[37] Y.N. Mu, F.N. Ding, P.N. Cui, J.Q. Ao, S.N. Hu, X.H. Chen, Transcriptome and expression profiling analysis revealed changes of multiple signaling pathways involved in immunity in the large yellow croaker during Aeromonas hydrophila infection, BMC Genomics 11 (2010) 506.
[38] D. Pietretti, G.F. Wiegertjes, Ligand specificities of Toll-like receptors in fish: indications from infection studies, Dev. Comp. Immunol. 43 (2) (2014) 205–222.
[39] A. Iwasaki, R. Medzhitov, Toll-like receptor control of the adaptive immune responses, Nat. Immunol. 5 (10) (2004) 987–995.
[40] P. Baoprasertkul, E. Peatman, J. Abernathy, Z. Liu, Structural characterisation and

expression analysis of toll-like receptor 2 gene from catfish, Fish Shellfish Immunol. 22 (4) (2007) 418–426.
[41] Y.C. Wei, T.S. Pan, M.X. Chang, et al., Cloning and expression of Toll-like receptors 1 and 2 from a teleost fish, the orange-spotted grouper Epinephelus coioides, Vet. Immunol. Immunopathol. 141 (2011) 173–182.
[42] Z.T. Qi, P. Wu, Q.H. Zhang, et al., Transcriptome analysis of soiny mullet (Liza haematocheila) spleen in response to Streptococcus dysgalactiae, Fish Shellfish Immunol. 49 (2016) 194–204.
[43] J. Hess, P. Angel, M. Schorpp-Kistner, AP-1 subunits: quarrel and harmony among siblings, J. Cell Sci. 117 (2004) 5965–5973.
[44] M. Ameyar, M. Wisniewska, J.B. Weitzman, A role for AP-1 in apoptosis: the case for and against, Biochimie 85 (8) (2003) 747–752.
[45] D. Gotthardt, H.J. Warnatz, O. Henschel, High-resolution dissection of phagosome maturation reveals distinct membrane trafficking phases, Mol. Biol. Cell 13 (10) (2002) 3508–3520.
[46] S. Keller, K. Berghoff, H. Kress, Phagosomal transport depends strongly on phagosome size, Sci. Rep. 7 (1) (2017) 17068.
[47] P.W. Gunning, U. Ghoshdastider, S. Whitaker, D. Popp, R.C. Robinson, The evolution of compositionally and functionally distinct actin filaments, J. Cell Sci. 128 (11) (2015) 2009–2019.
[48] G. Karp, K. Beginnen, S. Vogel, et al., Molekulare Zellbiologie, Springer, 978-3-540-23857-7, 2005.
[49] C.P. Samora, B. Mogessie, L. Conway, J.L. Ross, A. Straube, A.D. McAinsh, MAP4 and CLASP1 operate as a safety mechanism to maintain a stable spindle position in mitosis, Nat. Cell Biol. 13 (9) (2011) 1040–1050.
[50] T. Kiyomitsu, I.M. Cheeseman, Chromosome- and spindle-pole-derived signals generate an intrinsic code for spindle position and orientation, Nat. Cell Biol. 14 (3) (2012) 311–317.
[51] T. Bratkovic, M. Lunder, T. Popovic, et al., Affinity selection to papain yields potent peptide inhibitors of cathepsins L, B, H, and K, Biochem. Biophys. Res. Commun. 332 (3) (2005) 897–903.
[52] A. Savina, S. Amigorena, Phagocytosis and antigen presentation in dendritic cells, Immunol. Rev. 219 (1) (2007) 143–156.
[53] A. Aderem, Phagocytosis and the inflammatory response, J. Infect. Dis. 187 (s2) (2003) S340–S345.
[54] D. Valenzuela-Miranda, S. Boltaña, M.E. Cabrejos, et al., High-throughput transcriptome analysis of ISAV-infected Atlantic salmon Salmo salar unravels divergent immune responses associated to head-kidney, liver and gills tissues, Fish Shellfish Immunol 45 (2015) 367–377.
[55] C.A. Janeway, P. Travers, M. Walport, et al., Immunobiology: the Immune System in Health and Disease, fifth ed., Garland Science, New York, 2001.
[56] E. Peatman, Z. Liu, Evolution of CC chemokines in teleost fish: a case study in gene duplication and implications for immune diversity, Immunogenetics 59 (8) (2007) 613–623.